

~~CONFIDENTIAL~~

6
Copy
RM L54F03

NACA RM L54F03

NACA

RESEARCH MEMORANDUM

LIFT AND DRAG CHARACTERISTICS OF THE DOUGLAS D-558-II
RESEARCH AIRPLANE OBTAINED IN EXPLORATORY FLIGHTS TO
A MACH NUMBER OF 2.0

By Jack Nugent

Langley Aeronautical Laboratory

CLASSIFICATION ~~CHANGED~~ Langley Field, Va.

UNCLASSIFIED

LIBRARY COPY

To.....

NACA Reval effective
By authority of *FRN-128* Date *June 24, 1958*

AUG 5 1954

LANGLEY AERONAUTICAL LABORATORY
LIBRARY, NACA
LANGLEY FIELD, VIRGINIA

CLASSIFIED DOCUMENT

TM 8-13-58

This material contains information affecting the National Defense of the United States within the meaning of the espionage laws, Title 18, U.S.C., Secs. 793 and 794, the transmission or revelation of which in any manner to an unauthorized person is prohibited by law.

**NATIONAL ADVISORY COMMITTEE
FOR AERONAUTICS**

WASHINGTON

August 4, 1954

~~CONFIDENTIAL~~

NATIONAL ADVISORY COMMITTEE FOR AERONAUTICS

RESEARCH MEMORANDUM

LIFT AND DRAG CHARACTERISTICS OF THE DOUGLAS D-558-II
RESEARCH AIRPLANE OBTAINED IN EXPLORATORY FLIGHTS TO
A MACH NUMBER OF 2.0

By Jack Nugent

SUMMARY

A flight investigation was made of the 35° swept-wing D-558-II rocket-powered research airplane in the transonic and supersonic speed ranges. Lift and drag values obtained in exploratory flights of the basic configuration are presented.

As Mach number increased from 1.07 to 1.6 the value of lift-curve slope obtained for a lift-coefficient range of 0.2 to 0.5 decreased from a value of $0.066 \text{ degree}^{-1}$ to a value of $0.045 \text{ degree}^{-1}$. For a lift coefficient of about 0.2 and a Mach number range from 1.2 to 2.0 the drag coefficient remained constant at 0.09. For a lift coefficient of 0.3 the drag rise occurred at a Mach number of 0.85. For lift coefficients of 0.3 and 0.4 the drag coefficient increased to $\frac{3\frac{1}{2}}{2}$ times the respective subsonic values of 0.030 and 0.038. For the Mach number range from 1.2 to 1.6 the maximum lift-drag ratio was about 3.4 and occurred at lift coefficients in excess of 0.4. The drag-due-to-lift factor increased steadily from a value of 0.26 at a Mach number of 1.2 to a value of 0.33 at a Mach number of 1.6.

INTRODUCTION

The NACA High-Speed Flight Research Station is conducting flight measurements on the Douglas D-558-II rocket and turbojet-rocket swept-wing research airplanes through the transonic and supersonic speed ranges as part of the joint Air Force-Navy-NACA high-speed flight research program. This paper presents some lift and drag data obtained in these exploratory tests with the rocket-powered airplane at Mach numbers from 0.8 to 2.0. Most of the data were obtained for power-on

condition although some power-off data are included. The lift-coefficient range extended from about 0.3 to 0.7 for a Mach number of 0.8, but was less complete for other Mach numbers. For Mach numbers in excess of 1.6 there were data only for lift coefficients of 0.2, 0.225, and 0.3. The flights were made in the period from November 4 to December 23, 1953 at Edwards, Calif.

COEFFICIENTS AND SYMBOLS

A_e	exit area of nozzle, sq in.
A_t	throat area of nozzle, sq in.
a_N	normal acceleration, g units
a_X	measured longitudinal acceleration, g units
C_D	drag coefficient
C_L	lift coefficient
$C_{L\alpha}$	slope of lift curve, per deg
C_N	normal-force coefficient
C_n	rocket-nozzle coefficient
C_X	longitudinal-force coefficient
D	total drag, lb
dC_D/dC_L^2	drag-due-to-lift factor
F_n	net thrust, lb
g	acceleration due to gravity, ft/sec ²
L	lift, lb
L/D	lift-drag ratio

L/D_{\max}	maximum value of lift-drag ratio
M	free-stream Mach number
M.A.C.	mean aerodynamic chord, ft
p	static pressure, lb/sq in.
P_{c_a}	combustion chamber pressure, lb/sq in. absolute
P_{c_g}	combustion chamber pressure, lb/sq in. gage
P_e	exit pressure from rocket nozzle, lb/sq in. absolute
W	airplane weight, lb
α	angle of attack of airplane center line, deg
γ	angle between airplane flight path and horizontal, deg

AIRPLANE

The Douglas D-558-II airplanes have the 30-percent wing chord swept back 35° , sweptback tail surfaces, and an adjustable stabilizer for trim. The configuration included a constant-chord leading-edge slat fully retracted. The all-rocket airplane used in the present investigation employed a Reaction Motors LR8-RM-6 rocket engine equipped with nozzle extensions. The nozzle extensions were installed primarily to eliminate adverse rudder hinge-moment characteristics. They permitted the combustion gases to expand within the nozzle to pressure corresponding to an altitude of 27,000 feet instead of that corresponding to sea level. As a result the thrust increased from 7350 pounds to 7820 pounds at 60,000 feet. A three-view drawing of the subject airplane is shown in figure 1 and a photograph in figure 2. Pertinent airplane dimensions and characteristics are listed in table I.

INSTRUMENTATION

Standard NACA recording instruments were installed in the airplane to measure the following quantities pertinent to this investigation:

Airspeed
Altitude
Normal acceleration
Longitudinal acceleration
Angle of attack
Rocket cylinder combustion chamber pressure
Elevator and stabilizer positions

All of the instruments were synchronized by means of a common timer.

An NACA high-speed pitot-static head with a type A-6 (ref. 1) total pressure probe was mounted on a boom 57 inches forward of the nose of the airplane. The airspeed system was calibrated from $M = 0.6$ to $M = 2.0$ by the NACA radar phototheodolite method (ref. 2). The angle of attack was measured from a vane mounted on the nose boom and located 42 inches ahead of the apex of the airplane nose.

THRUST AND DRAG DETERMINATION

Thrust of the rocket engine was determined by use of the following equation for each chamber of the engine firing

$$F_n = p_{c_a} A_t C_n + A_e (p_e - p)$$

Atmospheric pressure p was added to chamber pressure p_{c_g} , obtained from a photopanel pressure gage, to obtain absolute pressure p_{c_a} . Exit pressure p_e was obtained by multiplying absolute chamber pressure by the expansion ratio p_e/p_{c_a} , which was determined theoretically from the measured throat and exit areas. The nozzle coefficients were determined from static thrust measurements on a thrust stand and checked in flight by comparing power-on and power-off data. There was little variation in the nozzle coefficients between cylinders permitting the use of an average value of 1.52 for all cylinders.

The accelerometer method was used to determine the drag forces (fig. 3) and the lift and drag coefficients were calculated by using the equations below:

$$C_D = C_X \cos \alpha + C_N \sin \alpha$$

$$C_L = C_N \cos \alpha - C_X \sin \alpha$$

ACCURACY

The following accuracies of measurement are applicable for the results presented herein:

α (position of vane), deg	± 0.2
α (overall), deg	± 1.0
a_N , g units	± 0.05
a_X , g units	± 0.01
F_n , lb	± 100

The nonobservational errors associated with the angle-of-attack measurements are floating angle of the vane, upwash over the airplane and nose boom, pitching velocity effects, and bending of the nose boom. Floating angle of the present test vane was not determined but data for comparable installations indicate that the floating-angle error can amount to as much as 0.5° for Mach numbers up to 1.10. (Refs. 3, 4, and unpublished data.) Error due to upwash over the airplane was shown to be of the order of 0.5° for the 35° swept-wing nose inlet airplane of reference 3 for a vane location comparable to the present test airplane, at a Mach number of 0.81 and a lift coefficient of 0.26. Reference 3 also shows that upwash over the airplane increases with lift coefficient and decreases with increasing transonic Mach numbers less than unity. For supersonic speeds upwash is theoretically zero. An analysis given in the above reference and applied to the vane-boom system here indicates an error due to upwash over the boom to be of the order of 1 percent. An investigation of errors due to pitching velocities showed that for the pitching velocities encountered any angle-of-attack correction due to this error source would be small. Bending of the boom results from inertia and aerodynamic loads which act in opposite directions. The magnitude of the boom bending at the angle-of-attack vane due to inertia had been determined by means of static loadings on the ground and was found to be 0.09° per g. The above correction was not used since its effects were small. From the above considerations it may be said that the overall error of measurement in angle of attack was of the order of 1° or less since some of the error sources are compensating.

The error in Mach number was within 0.01 at a Mach number of 0.7 and within 0.04 for a Mach number of 2.0.

The error in C_L was 5 percent or less throughout the lift range presented herein. The accuracy of the drag coefficient depends primarily upon the accuracies of thrust, angle of attack, longitudinal acceleration, and normal acceleration. By using the maximum estimated errors in thrust, longitudinal acceleration and normal acceleration the standard

deviation (defined in ref. 3) of the drag coefficient was calculated. The major portion of the data was within the dynamic pressure range of 147 to 407 pounds per square foot and for this range the standard deviation of the drag coefficient varied from 0.004 to 0.001, respectively. Angle-of-attack error was not included in the above analysis since it was not a random error. The effect of angle-of-attack errors would be to increase the values of the standard deviation of the drag coefficient presented.

TESTS, RESULTS, AND DISCUSSION

Lift and drag were determined for the Douglas D-558-II all-rocket airplane in the clean condition. The airplane was air-launched at about 30,000 feet from a Boeing B-29 mother airplane. Data were obtained over the altitude range of 30,000 to 70,000 feet during climbing flight, speed runs, and turns. The higher Mach numbers were obtained at altitudes in excess of 50,000 feet. Reynolds number varied from 5 to 17 million based on the wing mean aerodynamic chord. Use was made of the elevator and/or stabilizer during turns and for trim as found necessary by the pilot. Elevator position varied from 2.65° , trailing edge down, to 6° , trailing edge up, and stabilizer position varied from 3.35° , trailing edge down, to 5.08° , trailing edge up, for three of the four flights used for this paper. Data were not corrected for these control surface deflections.

Figure 4 presents the lift and drag characteristics for Mach numbers of 0.8, 1.07, 1.2, 1.3, and 1.6. The maximum Mach number variation was ± 0.05 since the drag variation with Mach number was not unduly large for the test Mach numbers. For a Mach number of 0.8 the highest lift coefficient obtained was about 0.7 and a distinct break occurred in the lift curve at a lift coefficient of about 0.65. For the supersonic Mach numbers the lift curves remained linear to lift coefficients of 0.5 to 0.7 which were the test limits. There were insufficient data obtained to establish fully any drag difference between power-on and power-off conditions.

The slopes of the lift curves for a lift-coefficient range from 0.2 to 0.5 are plotted against Mach number in figure 5. In the Mach number range from 1.07 to 1.6 the value of lift-curve slope decreased from a value of $0.066 \text{ degree}^{-1}$ to a value of $0.045 \text{ degree}^{-1}$.

Figure 6 shows the variation of drag coefficient with Mach number for constant values of lift coefficient. Drag levels were selected from the drag data of figure 4 at lift-coefficient values of 0.2, 0.3, and 0.4. The additional drag data cover a lift-coefficient variation of ± 0.01 from the specified lift coefficients of 0.2, 0.3, and 0.4. The isolated point

at Mach number of 2.0 with a drag-coefficient value of 0.092 is at a lift coefficient of 0.225. The Mach number range extended from 0.8 to 1.78 for a lift coefficient of 0.3 but was less complete for lift coefficients of 0.2 and 0.4. For a lift coefficient of 0.2 the Mach number range extended to 1.84. If the drag-rise Mach number is defined as the point where the variation of drag coefficient with Mach number reaches a value of 0.10, then for a lift coefficient of 0.30 the drag rise occurs at a Mach number of 0.85. From a Mach number of 1.20 to the test limits the drag coefficient remained approximately constant at 0.090, 0.104, and 0.123 for lift coefficients of 0.2, 0.3, and 0.4, respectively. The supersonic drag-coefficient level increased to about $3\frac{1}{2}$ times the subsonic drag levels of 0.030 and 0.038 for lift coefficients of 0.3 and 0.4, respectively.

Figure 7 shows the variation of lift-drag ratio with Mach number for the data of figure 6 and also shows the maximum lift-drag ratios for the five Mach numbers of figure 4. In the subsonic region there are insufficient flight data to determine the highest value of the maximum lift-drag ratio, whereas in the supersonic range the maximum lift-drag ratio drops to a value of about 3.4. The maximum lift-drag ratio occurs at a lift coefficient in excess of 0.4 in the Mach number range from 1.2 to 1.6.

Figure 8 presents the data of figure 4 plotted as drag coefficient against lift coefficient squared. Each curve shows a linear trend from the lowest lift coefficient shown to a lift coefficient at least as great as 0.5. Slopes were taken over the above lift-coefficient ranges and plotted against Mach number in figure 9. The value of the drag-due-to-lift factor increased steadily from a value of 0.26 at a Mach number of 1.2 to a value of 0.33 at a Mach number of 1.6.

CONCLUSIONS

Lift and drag measurements obtained in exploratory flights with the Douglas D-558-II rocket-powered swept-wing airplane over the Mach number range from 0.8 to 2.0 in the basic configuration led to the following conclusions:

1. As Mach number increased from 1.07 to 1.6 the value of lift-curve slope obtained for a lift-coefficient range from 0.2 to 0.5 decreased from a value of 0.066 degree⁻¹ to a value of 0.045 degree⁻¹.
2. For a lift coefficient of about 0.2 and a Mach number range from 1.2 to 2.0 the drag coefficient remained constant at 0.09. For a lift coefficient of 0.3 the drag rise occurred at a Mach number of 0.85.

For lift coefficients of 0.3 and 0.4 the drag coefficient increased to $3\frac{1}{2}$ times the respective subsonic values of 0.030 and 0.038.

3. For the Mach number range from 1.2 to 1.6 the maximum lift-drag ratio was about 3.4 and occurred at lift coefficients in excess of 0.4.

4. The drag-due-to-lift factor increased steadily from a value of 0.26 at a Mach number of 1.2 to a value of 0.33 at a Mach number of 1.6.

Langley Aeronautical Laboratory,
National Advisory Committee for Aeronautics,
Langley Field, Va., May 20, 1954.

REFERENCES

1. Gracey, William, Letko, William, and Russell, Walter R.: Wind-Tunnel Investigation of a Number of Total-Pressure Tubes at High Angles of Attack - Subsonic Speeds. NACA TN 2331, 1951. (Supersedes NACA RM L50G19.)
2. Zalovcik, John A.: A Radar Method of Calibrating Airspeed Installations on Airplanes in Maneuvers at High Altitudes and at Transonic and Supersonic Speeds. NACA Rep. 985, 1950. (Supersedes NACA TN 1979.)
3. McFadden, Norman M., Holden, George R., and Ratcliff, Jack W.: Instrumentation and Calibration Technique for Flight Calibration of Angle-of-Attack Systems on Aircraft. NACA RM A52I23, 1952.
4. Pearson, Albin O., and Brown, Harold A.: Calibration of a Combined Pitot-Static Tube and Vane-Type Flow Angularity Indicator at Transonic Speeds and at Large Angles of Attack or Yaw. NACA RM L52F24, 1952.

TABLE I

PHYSICAL CHARACTERISTICS OF THE DOUGLAS D-558-II AIRPLANE

Wing:

Root airfoil section (normal to 0.30 chord of unswept panel)	NACA 63-010
Tip airfoil section (normal to 0.30 chord of unswept panel)	NACA 63 ₁ -012
Total area, sq ft	175.0
Span, ft	25.0
Mean aerodynamic chord, in.	87.301
Root chord (parallel to plane of symmetry), in.	108.51
Extended tip chord (parallel to plane of symmetry), in.	61.18
Taper ratio	0.565
Aspect ratio	3.570
Sweep at 0.30 chord of unswept panel, deg	35.0
Sweep of leading edge, deg	38.8
Incidence at fuselage center line, deg	3.0
Dihedral, deg	-3.0
Geometric twist, deg	0
Total aileron area (rearward of hinge line), sq ft	9.8
Aileron travel (each), deg	±15
Total flap area, sq ft	12.58
Flap travel, deg	50

Horizontal tail:

Root airfoil section (normal to 0.30 chord of unswept panel)	NACA 63-010
Tip airfoil section (normal to 0.30 chord of unswept panel)	NACA 63-010
Total area, sq ft	39.9
Span, in.	143.6
Mean aerodynamic chord, in.	41.75
Root chord (parallel to plane of symmetry), in.	53.6
Extended tip chord (parallel to plane of symmetry), in.	26.8
Taper ratio	0.50
Aspect ratio	3.59
Sweep at 0.30 chord line of unswept panel, deg	40.0
Dihedral, deg	0
Elevator area, sq ft	9.4
Elevator travel, deg	
Up	25
Down	15
Stabilizer travel, deg	
Leading edge up	4
Leading edge down	5

TABLE I - Concluded

PHYSICAL CHARACTERISTICS OF THE DOUGLAS D-558-II AIRPLANE

Vertical tail:

Airfoil section (normal to 0.30 chord of unswept panel)	NACA 63-010
Effective area (area above root chord), sq ft	36.6
Height from fuselage reference line, in.	98.0
Root chord (chord 24 in. above fuselage reference line), in.	116.8
Extended tip chord (parallel to fuselage reference line), in.	27.0
Sweep angle at 0.30 chord of unswept panel, deg	49.0
Rudder area (aft hinge line), sq ft	6.15
Rudder travel, deg	±25

Fuselage:

Length, ft	42.0
Maximum diameter, in.	60.0
Fineness ratio	8.40
Speed-retarder area, sq ft	5.25

Power plant:

Rocket	LR8-RM-6
------------------	----------

Airplane weight, lb:

Full rocket fuel	15,787
No fuel.	9,421

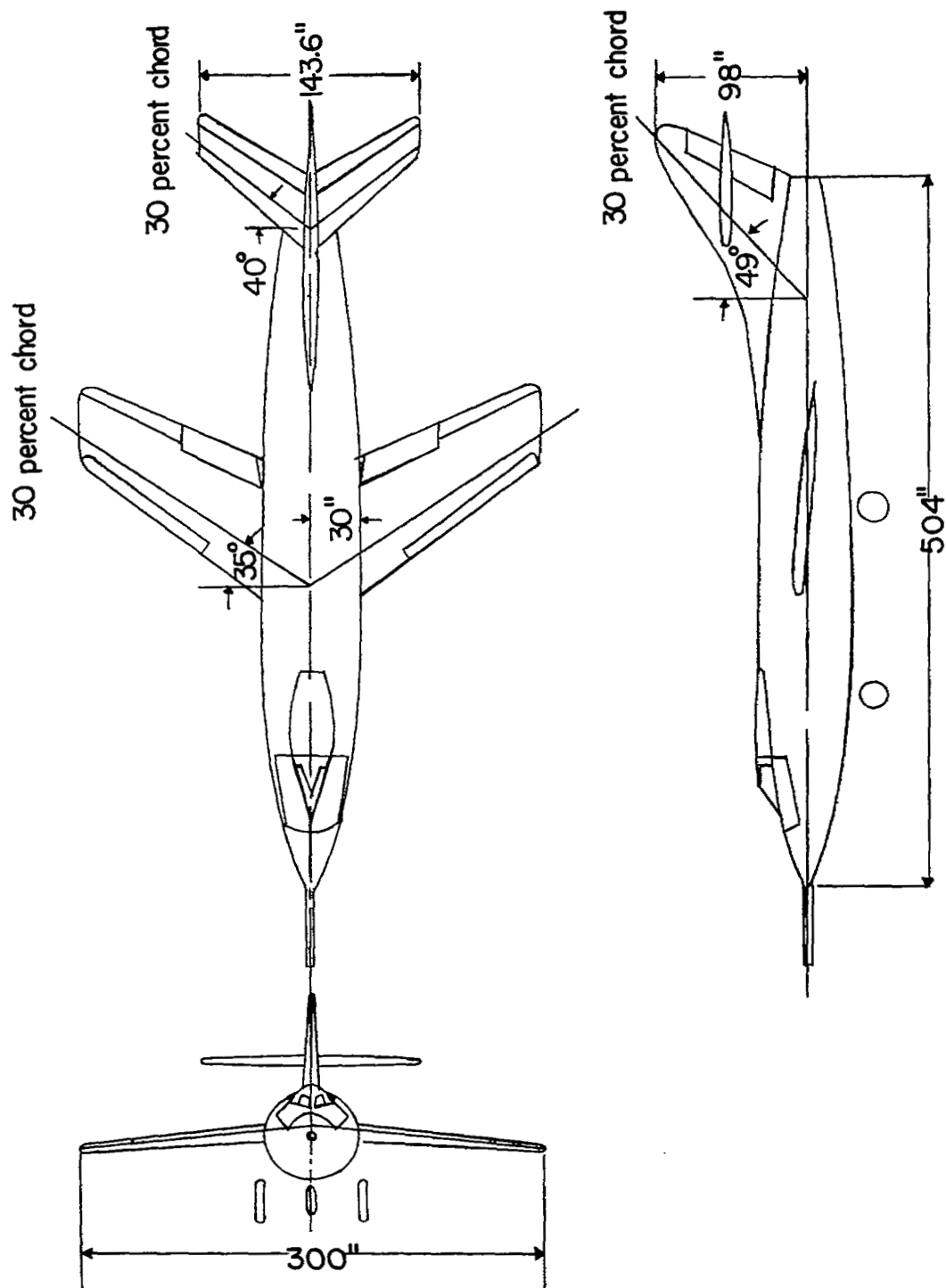


Figure 1.- Three-view drawing of the D-558-II research airplane.



L-73282.1

Figure 2.- Three-quarter front view of the Douglas D-558-II research airplane.

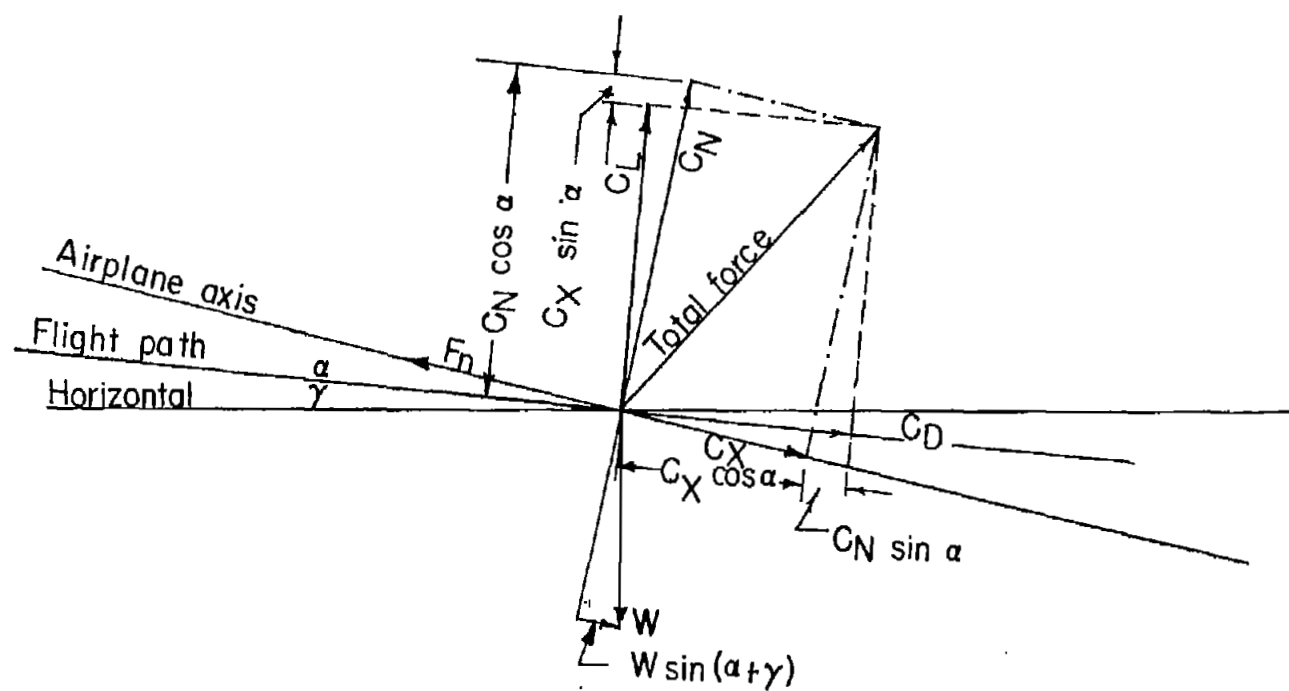


Figure 3.- Method of calculating lift and drag coefficients.

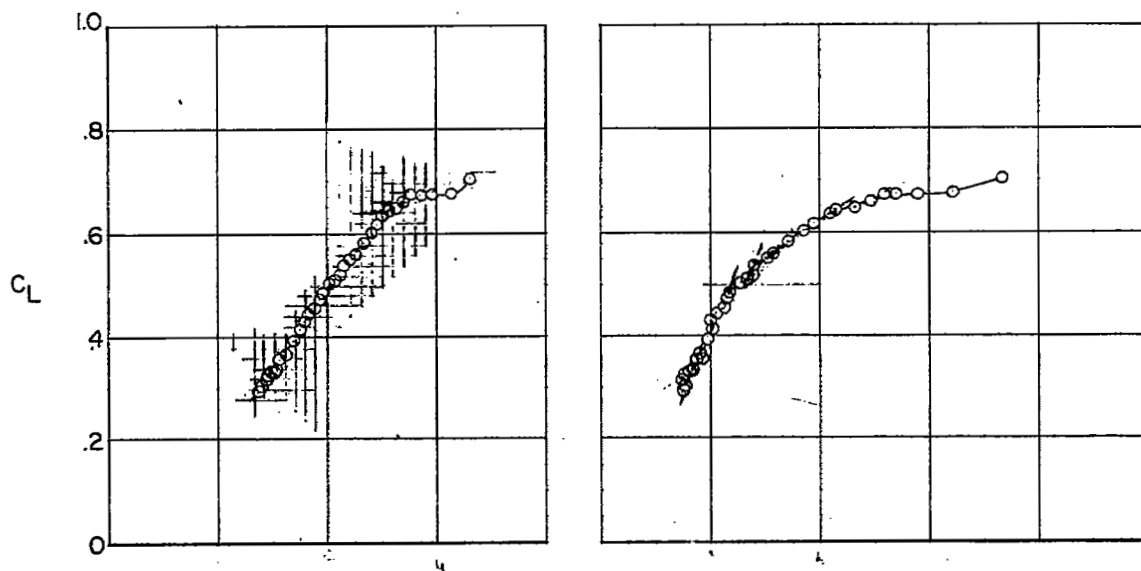
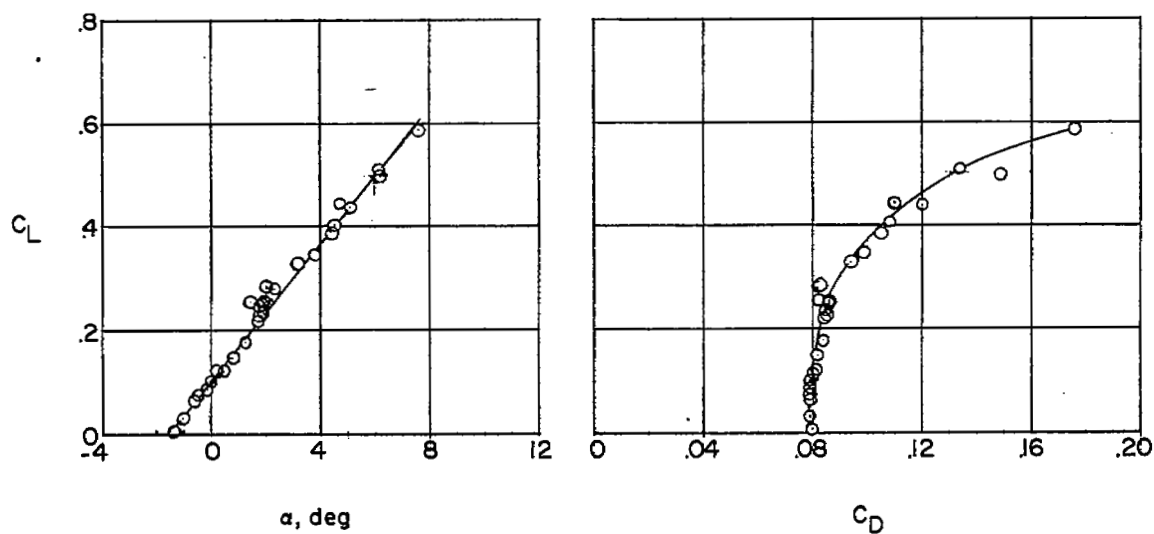
(a) $M = 0.800 \pm 0.025$.(b) $M = 1.07 \pm 0.02$.

Figure 4.- Lift and drag characteristics obtained during climbing flight, speed runs, and turns for the D-558-II research airplane.

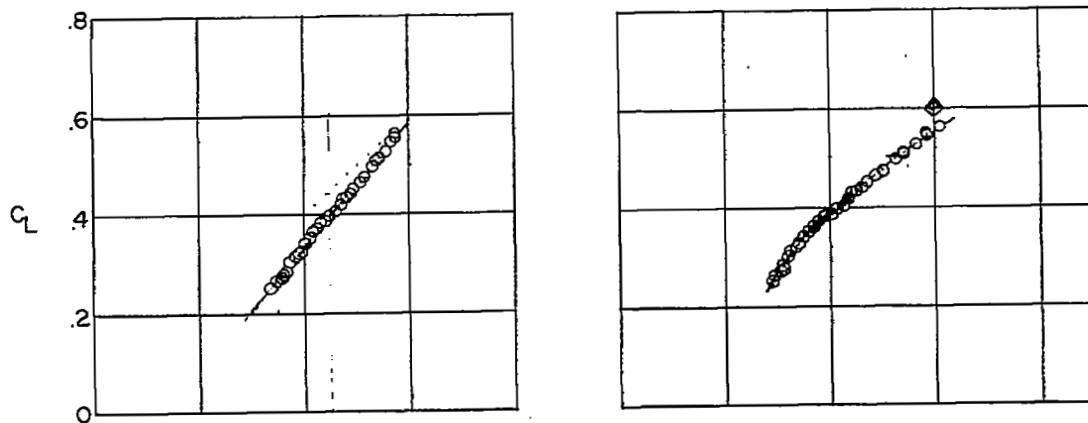
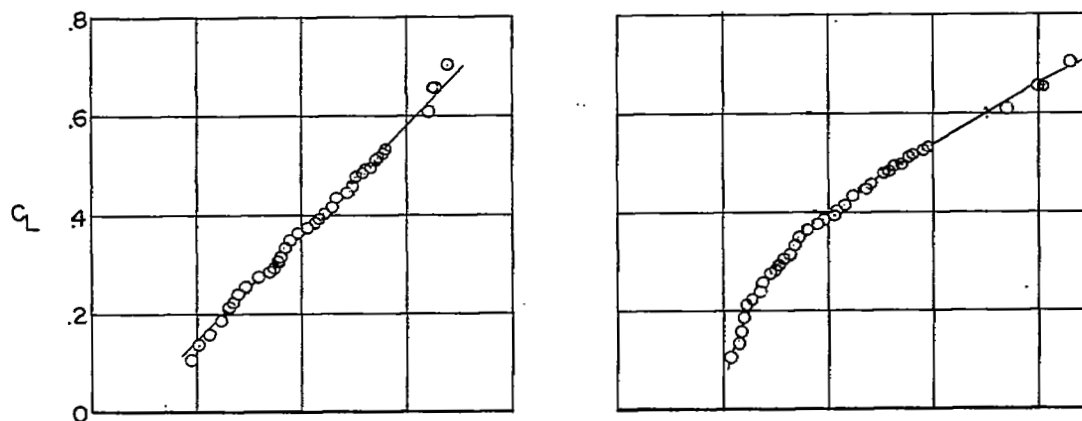
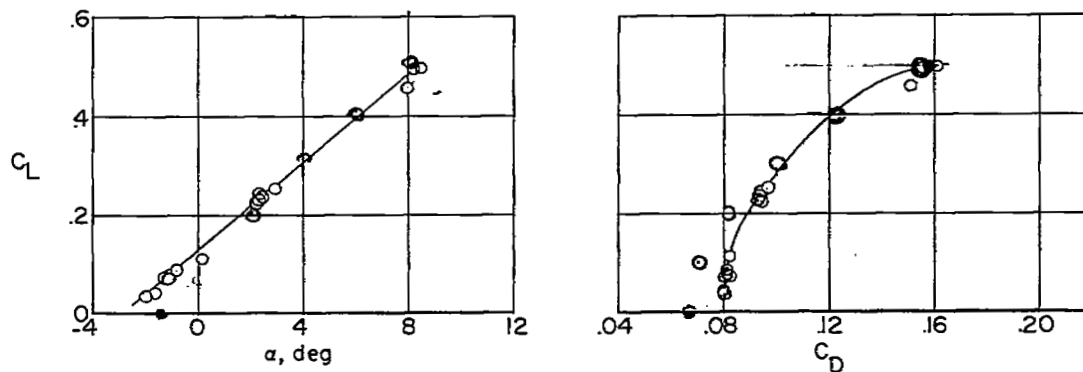
(c) $M = 1.20 \pm 0.05$.(d) $M = 1.30 \pm 0.05$.(e) $M = 1.60 \pm 0.05$.

Figure 4.- Concluded.

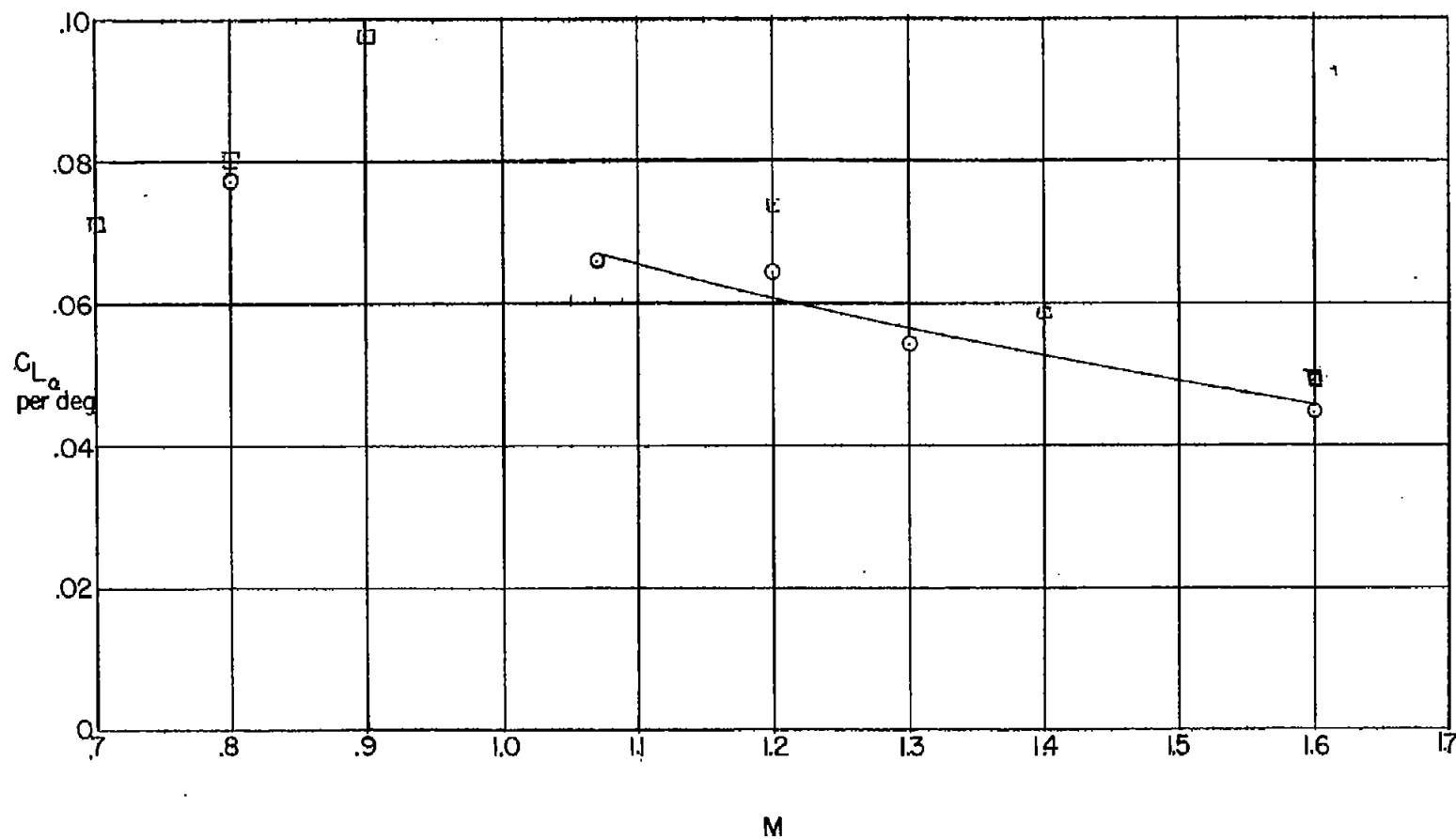


Figure 5.- Variation of lift-curve slope with Mach number.

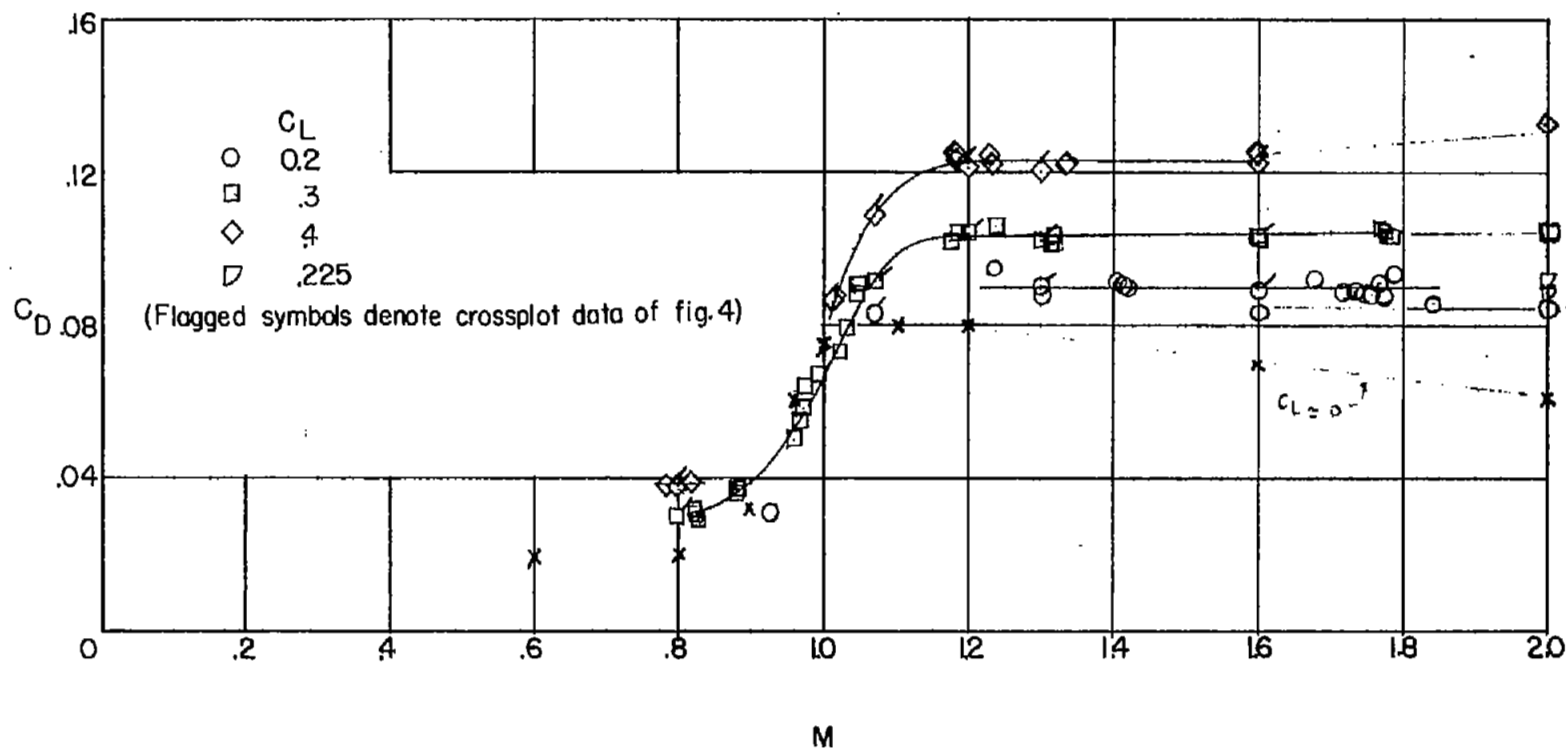


Figure 6.- Variation of drag coefficient with Mach number for constant values of lift coefficient.

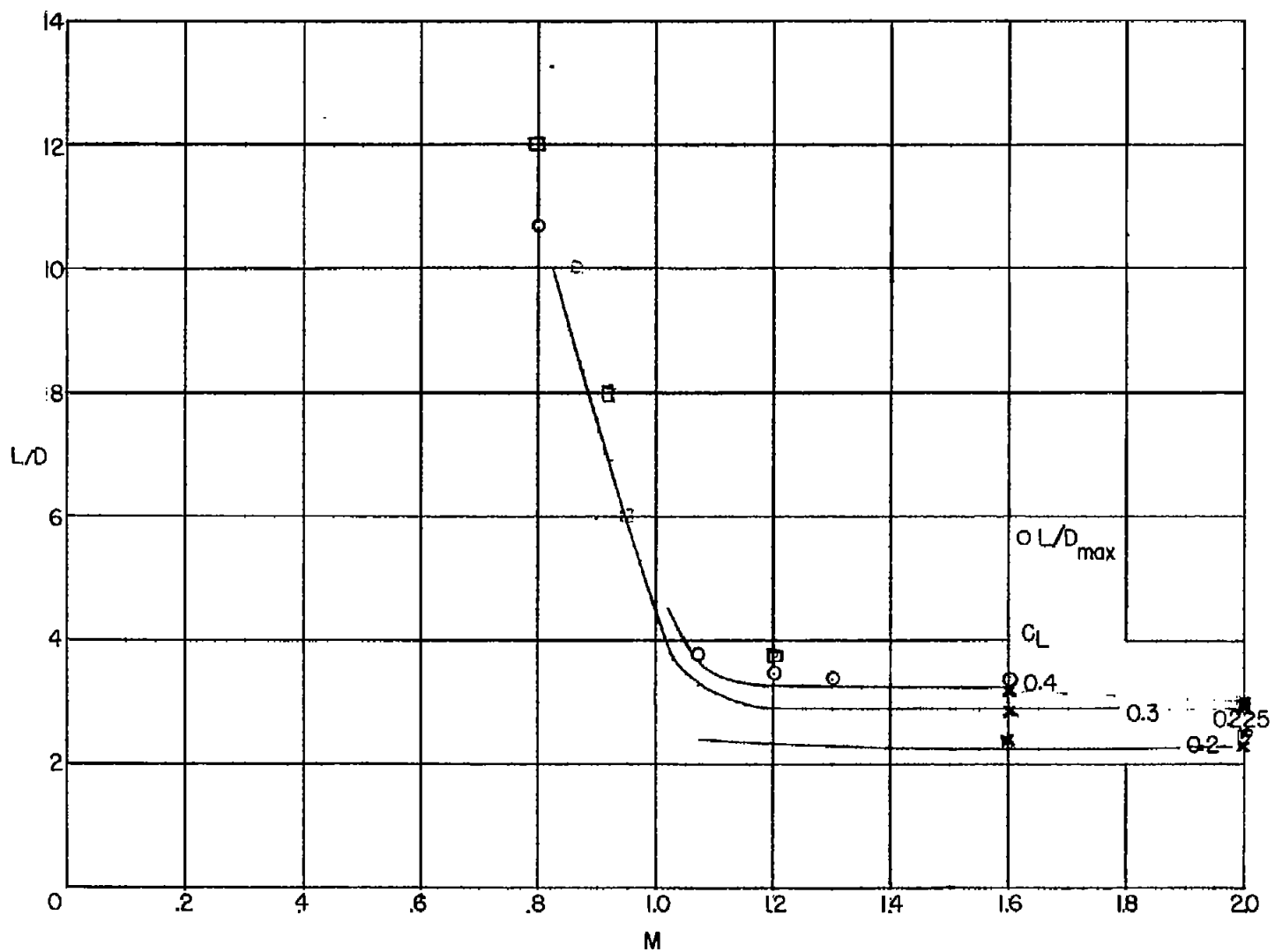


Figure 7.- Variation of lift-drag ratio with Mach number.

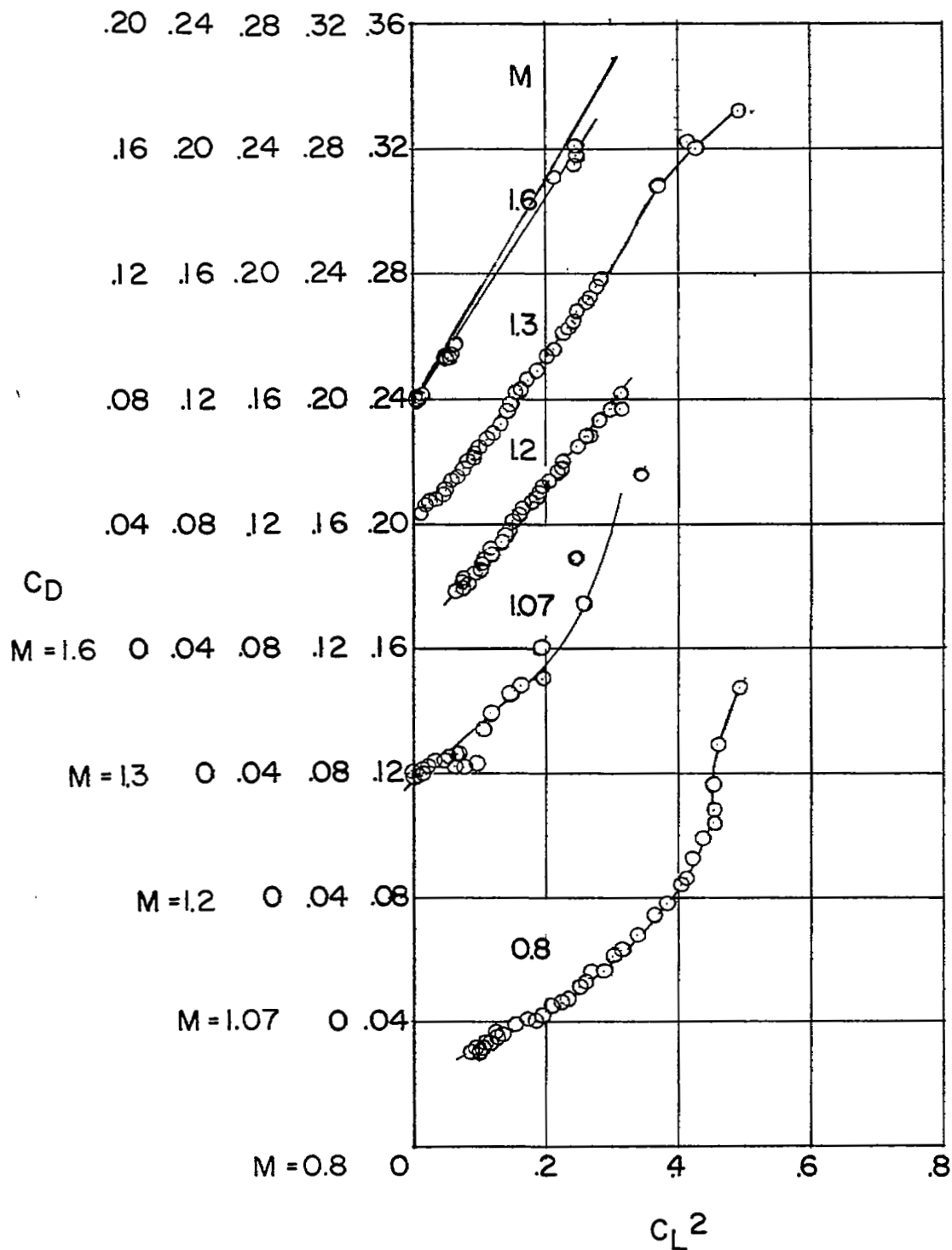


Figure 8.- Variation of drag coefficient with lift coefficient squared.

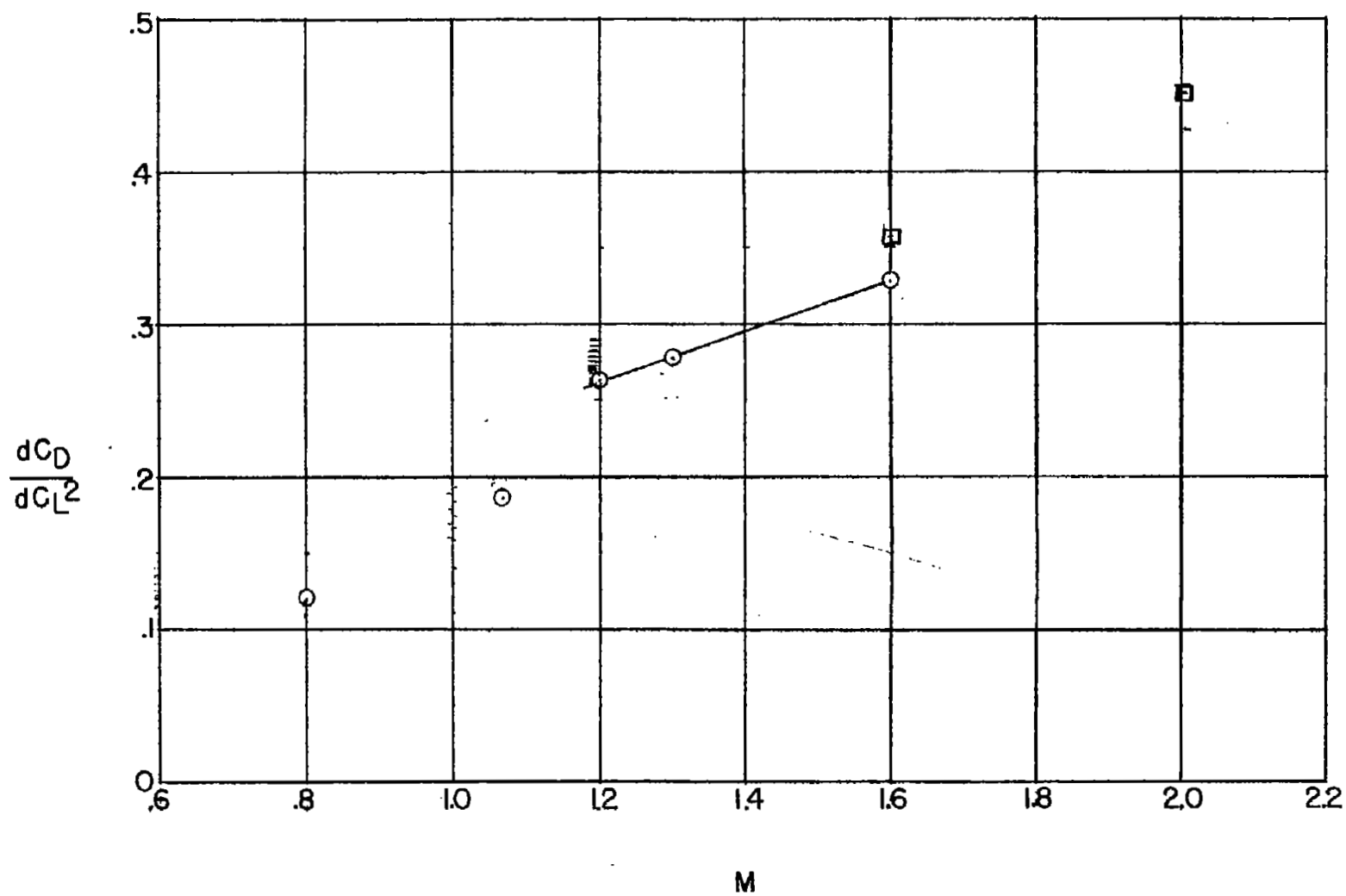



Figure 9.- Variation of drag-due-to-lift factor with Mach number.

[REDACTED]

LANGLEY RESEARCH CENTER



3 1176 00516 8001

1
1

1
1

1
1

[REDACTED]